Searching for new physics from SMEFT and leptoquarks at the P2 experiment

Ingolf Bischer and Werner Rodejohann
Max-Planck-Institut für Kernphysik, Saupfercheckweg 1, 69117 Heidelberg, Germany

P. S. Bhupal Dev
Department of Physics and McDonnell Center for the Space Sciences, Washington University, St. Louis, Missouri 63130, USA

Xun-Jie Xu
Institute of High Energy Physics, Chinese Academy of Sciences, Beijing 100049, China

Yongchao Zhang
School of Physics, Southeast University, Nanjing 211189, China

(Received 16 February 2022; accepted 25 April 2022; published 16 May 2022)

The P2 experiment aims at high-precision measurements of the parity-violating asymmetry in elastic electron-proton and electron-^{12}C scatterings with longitudinally polarized electrons. We discuss here the sensitivity of P2 to leptoquarks, which within the P2 energy range can be described in the language of Standard Model effective field theory (SMEFT). We give the expected P2 limits on the SMEFT operators and on the leptoquark parameters, which will test energy scales up to 15 TeV. In many cases those limits exceed current constraints from LHC and atomic parity violation (APV) experiments. We also demonstrate that degeneracies of different SMEFT operators can partially be resolved by use of APV experiments and different targets (protons and ^{12}C) at P2. Moreover, we show that P2 could confirm or resolve potential tensions between the theoretical and experimental determinations of the weak charge of ^{133}Cs.

DOI: 10.1103/PhysRevD.105.095016

I. INTRODUCTION

Leptoquarks are colored scalar or vector particles that couple to the quarks and leptons of the Standard Model (SM), see Ref. [1] for a review. They arise in many theories beyond the SM, including grand unified theories [2–9], string and M-theories [10], R-parity-violating supersymmetry [11] and radiative neutrino mass models [12–16]. They are frequently used candidates to explain the current anomalies in the muon anomalous magnetic moment and in semileptonic B-decays [17–65]; see Ref. [66] for a review. In general, the quantum numbers of leptoquarks are governed by the quantum numbers of SM particles involved [67]. As the SM is a chiral theory, hence violates parity, leptoquarks can be expected to influence measurable parity violation. More generally, parity-violating interactions at low-energy scales from new physics at large mass scales can be described by operators of SM effective field theory (SMEFT) [68,69].

In this paper we focus on the P2 experiment, which will measure the parity-asymmetry in elastic electron-proton or electron-^{12}C scatterings at the upcoming Mainz Energy-recovering Superconducting Accelerator (MESA) facility [70]. The crucial observable is the parity violating cross section asymmetry $(\sigma_L - \sigma_R)/(\sigma_L + \sigma_R)$ for the scattering of longitudinally polarized electrons off the targets. The expectation is that the SM parity asymmetry can be measured with 1.4% (0.3%) relative uncertainty for a proton (^{12}C) target, which can be used to constrain beyond SM contributions [70,71]. Our goal in this paper is to use these expected values to set prospective limits on SMEFT coefficients and leptoquark masses and couplings to first-generation SM fermions.

As the momentum exchange relevant for P2 is less than 100 MeV [70] which is very small compared to the allowed mass of leptoquarks, one can approximate their interactions in terms of effective SMEFT operators. Hence, we start by obtaining the prospective limits on relevant SMEFT operators in Table III and Table IV, which can be translated into constraints on specific models inducing these operators, as

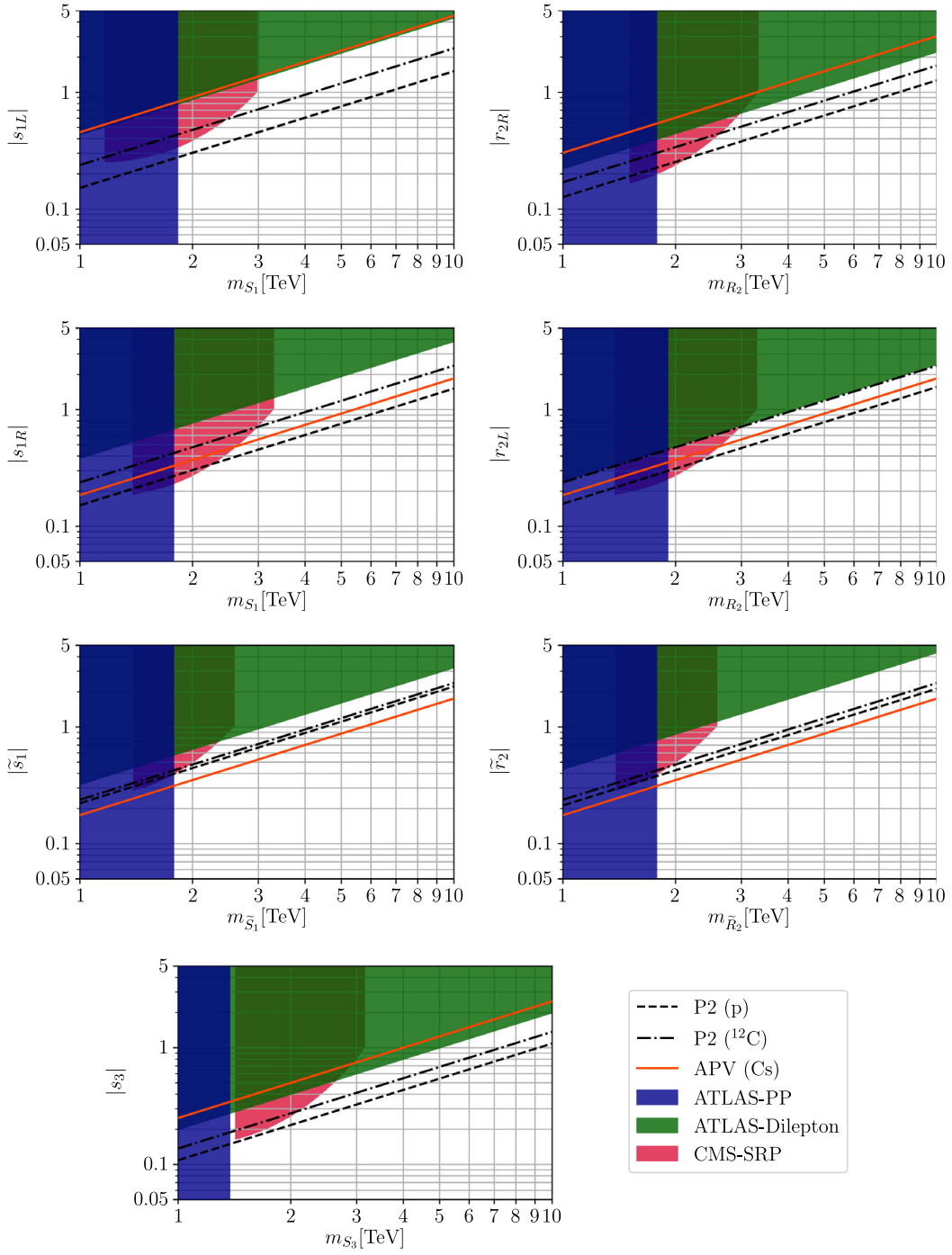

FIG. 1. Expected 95% CL exclusion limits from P2 for scalar leptoquarks assuming one coupling to dominate, compared to existing bounds from APV [72] and the LHC limits from pair production (PP) [73,74], dilepton [75] and single resonant production (SRP) [76] channels. The constant ratios $m_{\mathrm{LQ}}/g_{\mathrm{LQ}}$ from P2, APV and ATLAS-Dilepton correspond to the entries of Table V.

shown in Table V. Subsequently, we use the identification with SMEFT operators to map out expected bounds on leptoquark parameters. We confront those leptoquark bounds with current constraints, most notably from atomic parity violation (APV) using ^{133}Cs [72] and from leptoquark production at the LHC in the pair-production [73,74], Drell-Yan [75] and single resonant production [76] channels. As we will show in Figs. 1 and 2, in many cases the P2 limits will supersede current constraints, if the mass of the leptoquark exceeds roughly 2 TeV. We also confirm that certain SMEFT operators lead to an indistinguishable effect in a given observable. In this case one can partially resolve this degeneracy by taking advantage of the fact that different observables use different amounts of up- and

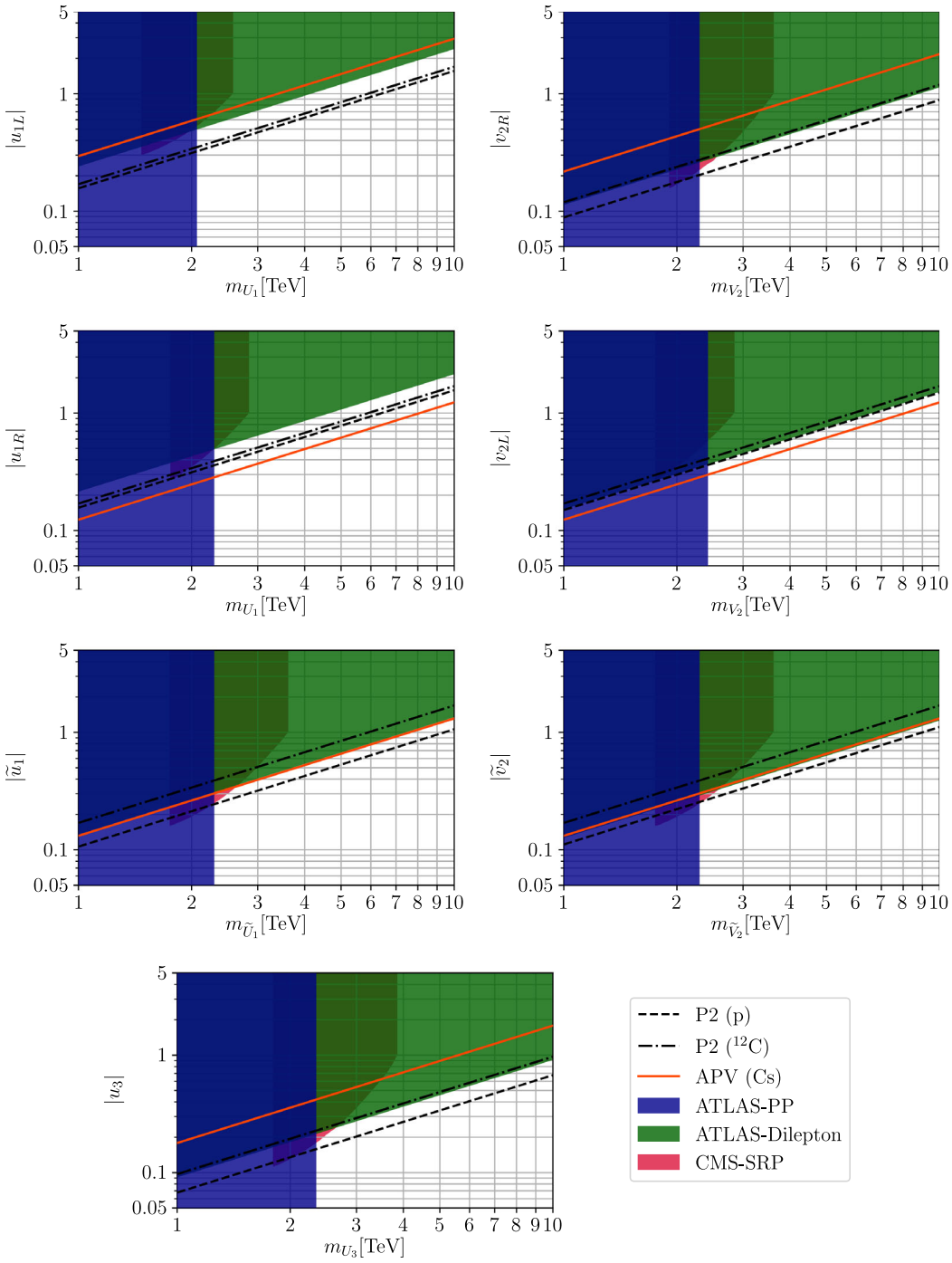

FIG. 2. Expected 95% CL exclusion limits from P2 for vector leptoquarks assuming one coupling to dominate, compared to existing bounds from APV [72] and the LHC limits from pair production (PP) [73,74], dilepton [75] and single resonant production (SRP) [76] channels. The constant ratios $m_{\mathrm{LQ}}/g_{\mathrm{LQ}}$ from P2, APV and ATLAS-Dilepton correspond to the entries of Table V.

down-quarks in the target material, as illustrated in Fig. 3. We therefore stress the complementarity of using protons and ^{12}C at P2, as well as ^{133}Cs in APV to better disentangle up- and down-quark interactions.

We note that there have been a number of studies on low-energy parity violating effects of new physics [77–84] and in particular on the P2 sensitivity to new physics [71,85]. While Ref. [71] focuses on low-mass gauge bosons and Ref. [85] considers broadly a variety of constraints from low-energy observables to collider searches, this work presents a dedicated study on the P2 sensitivity to new physics that can be handled via the

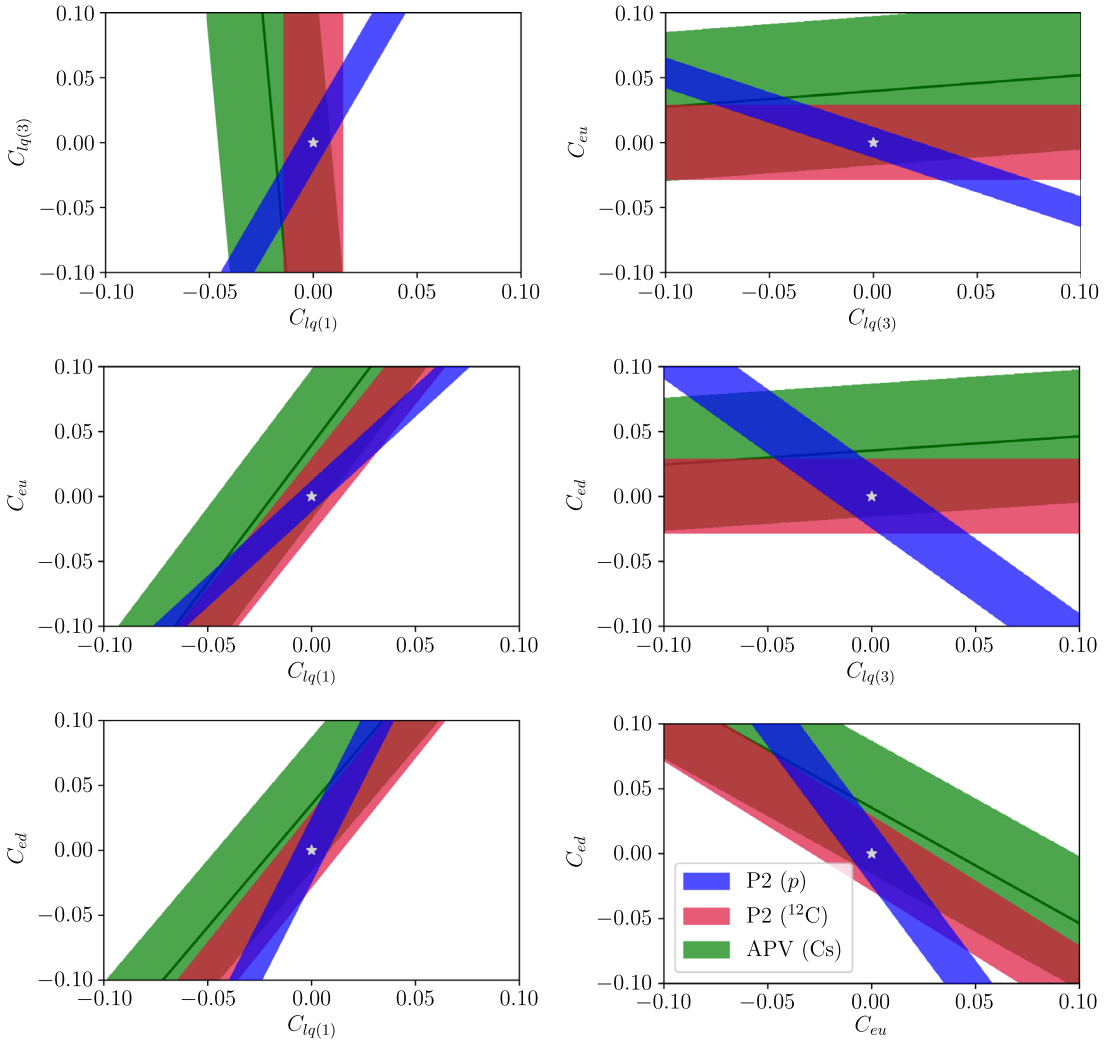

FIG. 3. Expected exclusion limits from P2 considering two SMEFT coefficients at a time, compared with existing measurement from APV [72]. The SM expectation is marked by an asterisk and the best fit to APV is shown as a dark green line. The EFT scale Λ is set to 1 TeV.

SMEFT, with an application to the leptoquark scenario. Our main new observation is the importance of using ^{12}C target to break the degeneracy between up- and down-quark couplings.

The rest of the paper is organized as follows. In Sec. II we lay out the formalism of SMEFT operators and leptoquarks with focus on parity violation in the first generation. In Sec. III we map the fundamental quark-level couplings to nucleon and nucleus couplings, calculate the parity asymmetry and set limits on SMEFT energy scales and leptoquark masses. Section IV compares those limits to current ones from APV and LHC. The advantage of using different targets is illustrated in Sec. V by taking two effective couplings at a time. Our conclusions are presented in Sec. VI. Mapping of the SMEFT coefficients to the flavor basis is done in Appendix A, and the parametrization of the form factors is presented in Appendix B.

II. HIGH-ENERGY ORIGINS OF PARITY VIOLATION IN ELECTRON-HADRON SCATTERING

New physics at large mass scales may lead to deviations from the expected parity violation at scattering experiments. In this section, we describe two frequently investigated scenarios of new physics. The first is the model-independent approach of parametrizing new physics as effective operators in the SMEFT. The second approach is considering minimal scenarios of leptoquarks as explicit particle extensions of the SM.

A. Standard Model effective field theory

If one considers new physics at some high mass scale $\Lambda \gg m_W$, a suitable framework to encode different possible effects at energies well below that scale is given by effective field theories. For the SM it is convenient to apply SMEFT

[86]. Besides the SM Lagrangian, this effective theory consists of a series of nonrenormalizable operators of higher mass-dimension $d \geq 5$, such that we can write

$$\mathcal{L}_{\text{eff}} = \mathcal{L}_{\text{SM}} + \sum_i \sum_{n\geq 5} \frac{1}{\Lambda^{n-4}} C_i \mathcal{O}_i^{(n)}, \tag{1}$$

where C_i denotes the dimensionless Wilson coefficient of the operator $\mathcal{O}_i$ defined, e.g., in Refs. [68,69]. Operators of dimension $4+n$ are suppressed by respective factors of Λ^{-n}. This expansion is supposed to be applicable at interaction energies $q^2 \ll \Lambda^2$, while new particles associated with Λ may only be produced on-shell at much higher energy scales.

The SMEFT operators of lowest dimension giving rise to $eeuu$ or $eedd$ interactions relevant at the P2 experiment are, in the usual terminology [69], the parity-violating operators[1] $\mathcal{O}_{lq(1)}$, $\mathcal{O}_{lq(3)}$, $\mathcal{O}_{lu}$, $\mathcal{O}_{ld}$, $\mathcal{O}_{qe}$, $\mathcal{O}_{eu}$, $\mathcal{O}_{ed}$, and the parity-conserving operators $\mathcal{O}_{ledq}$, $\mathcal{O}_{lequ(1)}$, and $\mathcal{O}_{lequ(3)}$. Starting with the parity-violating operators the effective Lagrangian can be written as

$$\mathcal{L}_{\text{PV}} = \frac{1}{\Lambda^2} \sum_{f=u,d} \sum_{X=L,R} (\bar{e}\gamma_\mu P_X e) \times [C_{XVf}(\bar{f}\gamma^\mu f) + C_{XAf}(\bar{f}\gamma^\mu\gamma^5 f)], \tag{2}$$

where e, u, and d denote electron, up quark, and down quark mass eigenstates. The chirality projectors are given by $P_{L,R} = \frac{1}{2}(1 \mp \gamma_5)$. The coefficients C_{XYf} are related to the coefficients of SMEFT operators in the mass basis via

$$C_{LVu} = \frac{1}{2}(C_{lq(1)} - C_{lq(3)} + C_{lu}), \tag{3a}$$

$$C_{LVd} = \frac{1}{2}(C_{lq(1)} + C_{lq(3)} + C_{ld}), \tag{3b}$$

$$C_{LAu} = \frac{1}{2}(-C_{lq(1)} + C_{lq(3)} + C_{lu}), \tag{3c}$$

$$C_{LAd} = \frac{1}{2}(-C_{lq(1)} - C_{lq(3)} + C_{ld}), \tag{3d}$$

$$C_{RVu} = \frac{1}{2}(C_{qe} + C_{eu}), \tag{3e}$$

$$C_{RVd} = \frac{1}{2}(C_{qe} + C_{ed}), \tag{3f}$$

$$C_{RAu} = \frac{1}{2}(-C_{qe} + C_{eu}), \tag{3g}$$

$$C_{RAd} = \frac{1}{2}(-C_{qe} + C_{ed}), \tag{3h}$$

where first-generation indices $ee11$ are implied. For a mapping to the flavor basis, see Appendix A. The parity-conserving scalar and tensor interactions read

$$\mathcal{L}_{\text{PC}} = \frac{1}{\Lambda^2} \sum_{f=u,d} (\bar{e}P_L e)[C_{Sf}(\bar{f}f) + C_{Pf}(\bar{f}\gamma^5 f)] + (\bar{e}\sigma_{\mu\nu}P_L e)[C_{Tf}\bar{f}\sigma^{\mu\nu}P_L f] + \text{H.c.}, \tag{4}$$

with the mass-basis coefficients

$$C_{Su} = C_{Pu} = -\frac{1}{2}C_{lequ(1)}, \tag{5a}$$

$$C_{Sd} = -C_{Pd} = \frac{1}{2}C_{ledq}, \tag{5b}$$

$$C_{Tu} = -C_{lequ(3)}, \tag{5c}$$

$$C_{Td} = 0. \tag{5d}$$

We have checked that these definitions are consistent with previous investigations of parity violation from SMEFT [88]. Since (pseudo)scalar and tensor interactions are parity-conserving, the P2 sensitivity of these interactions is poor compared to other probes. For this reason we focus on the parity-violating vector and axial vector interactions.

TABLE I. Leptoquarks along with their quantum numbers investigated in this work. We use the convention where electric charge $Q = I_3 + Y$ with weak isospin component I_3 and hypercharge Y; $F = 3B + L$ denotes fermion number, with baryon number B and lepton number L.

	$F = 3B + L$	Spin	SU(3)_C	SU(2)_L	U(1)_Y
S_1	2	0	3	1	−1/3
$\tilde{S}_1$	2	0	3	1	−4/3
S_3	2	0	3	3	−1/3
V_2	2	1	3	2	−5/6
$\tilde{V}_2$	2	1	3	2	1/6
R_2	0	0	3	2	7/6
$\tilde{R}_2$	0	0	3	2	1/6
U_1	0	1	3	1	2/3
$\tilde{U}_1$	0	1	3	1	5/3
U_3	0	1	3	3	2/3

B. Leptoquarks

Leptoquarks are hypothetical scalar or vector particles which generically contribute to parity-violating interactions. In this work we follow the naming convention of Ref. [67] and consider all leptoquarks which can give rise to effective quark-electron interactions. These are

[1]Other works on the parity-violating operators can be found, e.g., in Refs. [87,88].

listed, along with their quantum numbers, in Table I. For convenience, we write all of them as fundamental representations of $SU(3)_C$.

The contributions to the parity-violating SMEFT operators from integrating out heavy leptoquarks read

$$C_{lq(1)} = -\frac{1}{4}|s_{1L}|^2 - \frac{3}{4}|s_3|^2 + \frac{1}{2}|u_{1L}|^2 + \frac{3}{2}|u_3|^2, \quad (6a)$$

$$C_{lq(3)} = +\frac{1}{4}|s_{1L}|^2 - \frac{1}{4}|s_3|^2 + \frac{1}{2}|u_{1L}|^2 - \frac{1}{2}|u_3|^2, \quad (6b)$$

$$C_{eu} = -\frac{1}{2}|s_{1R}|^2 + |\tilde{u}_1|^2, \quad (6c)$$

$$C_{ed} = -\frac{1}{2}|\tilde{s}_1|^2 + |u_{1R}|^2, \quad (6d)$$

$$C_{qe} = \frac{1}{2}|r_{2R}|^2 - |v_{2R}|^2, \quad (6e)$$

$$C_{lu} = \frac{1}{2}|r_{2L}|^2 - |\tilde{v}_2|^2, \quad (6f)$$

$$C_{ld} = \frac{1}{2}|\tilde{r}_2|^2 - |v_{2L}|^2, \quad (6g)$$

where we have identified $\Lambda = m_{\rm LQ}$ (the same for all leptoquarks). The couplings are defined through the interaction Lagrangians

$$\begin{aligned}\mathcal{L}_{F=2} = {} & (s_{1L}\bar{q}^a\epsilon^{ab}(l^c)^b + s_{1R}\overline{u_R}e_R^c)S_1 \\ & + \tilde{s}_1\overline{d_R}e^c\tilde{S}_1 + s_3\bar{q}^a(\vec{\tau})^{ab}\epsilon^{bd}(l^c)^d\vec{S}_3 \\ & + (v_{2R}\bar{q}^a\gamma_\mu e_R^c + v_{2L}\bar{d}_R\gamma_\mu(l^c)^a)V_2^{\mu,a} \\ & + \tilde{v}_2\overline{u_R}\gamma_\mu(l^c)^a\tilde{V}_2^{\mu,a} + \text{H.c.}, \end{aligned} \quad (7a)$$

$$\begin{aligned}\mathcal{L}_{F=0} = {} & (r_{2R}\bar{q}^b e_R + r_{2L}\overline{u_R}l^a\epsilon^{ab})R_2^b + (\tilde{r}_2\overline{d_R}l^a\epsilon^{ab})R_2^{b\prime} \\ & + (u_{1L}\bar{q}\gamma_\mu l + u_{1R}\overline{d_R}\gamma_\mu e_R)U_1^\mu \\ & + \tilde{u}_1\overline{u_R}\gamma_\mu e_R U_1^{\mu\prime} + u_3\bar{q}\,\vec{\tau}\,\gamma_\mu l\vec{U}_3^\mu + \text{H.c.}, \end{aligned} \quad (7b)$$

where a, b denote $SU(2)_L$ indices, ϵ^{ab} is the Levi-Civita symbol, and $\vec{\tau} = (\tau_1, \tau_2, \tau_3)$ are the Pauli matrices. Generally, we refer to any single mass by $m_{\rm LQ}$ and any single coupling by $g_{\rm LQ}$.

Collider searches have ruled out leptoquarks of masses below about 1.8 TeV, as discussed in Sec. IV B. Therefore, we can focus on a regime where the full leptoquark propagators can be approximated using $|q^2| \ll m_{\rm LQ}^2$:

$$G_{\mu\nu}^{\rm vector}(q) = i\frac{-g_{\mu\nu} + \frac{q_\mu q_\nu}{m_{\rm LQ}^2}}{q^2 - m_{\rm LQ}^2} \approx ig_{\mu\nu}\frac{1}{m_{\rm LQ}^2}, \quad (8a)$$

$$G^{\rm scalar}(q) = i\frac{1}{q^2 - m_{\rm LQ}^2} \approx -i\frac{1}{m_{\rm LQ}^2}. \quad (8b)$$

Therefore, for large leptoquark masses P2 is sensitive to the combination $g_{\rm LQ}/m_{\rm LQ}$.

III. SETTING CONSTRAINTS

A. Mapping fundamental couplings to nucleon and nucleus couplings

In order to connect the fundamental couplings with quarks to those with protons or, more generally, with nuclei, we need to apply the nuclear matrix elements and introduce form factors. Following the usual convention explained e.g., in Ref. [89], we write for the vector and axial-vector currents

$$\begin{aligned}&\langle N(p')|\bar{f}\gamma^\mu f|N(p)\rangle \\ &\quad = \bar{u}(p')\left[F_1^{f,N}(q^2)\gamma^\mu + F_2^{f,N}(q^2)\frac{i\sigma^{\mu\nu}q_\nu}{2m_N}\right]u(p), \end{aligned} \quad (9a)$$

$$\begin{aligned}&\langle N(p')|\bar{f}\gamma^\mu\gamma^5 f|N(p)\rangle \\ &\quad = \bar{u}(p')\left[G_A^{f,N}(q^2)\gamma^\mu\gamma^5 + G_P^{f,N}(q^2)\frac{\gamma^5 q^\mu}{2m_N}\right]u(p), \end{aligned} \quad (9b)$$

where $q = p_e - k_e$ is the difference of initial and final state electron momenta, $f = u$, d, s (note that we include s quarks) and $N = p$, n for nucleons. Assuming isospin symmetry, the form factors related to the vector matrix element can be related to the electromagnetic Dirac and Pauli form factors F_1^N and F_2^N as

$$F_i^{u,p} = F_i^{d,n} = 2F_i^p + F_i^n + F_i^{s,p}, \quad (10a)$$

$$F_i^{d,p} = F_i^{u,n} = F_i^p + 2F_i^n + F_i^{s,p}. \quad (10b)$$

The form factors F_i^N can be rewritten in terms of the electric and magnetic Sachs form factors G_E^N and G_M^N as

$$F_1^N(q^2) = \frac{G_E^N(q^2) - \frac{q^2}{4m_N^2}G_M^N(q^2)}{1 - q^2/4m_N^2}, \quad (11a)$$

$$F_2^N(q^2) = \frac{G_M^N(q^2) - G_E^N(q^2)}{1 - q^2/4m_N^2}. \quad (11b)$$

The same holds true for the strange form factors $F_i^{s,p}$ which can be expressed in terms of Sachs form factors G_E^s and G_M^s analogous to Eq. (11). We use the same parametrization of the form factors as Ref. [70]. Details are given in Appendix B. Turning to the axial form factors, we take [89]

$$G_A^{q,N} = \Delta_q^{(N)}, \quad (12a)$$

$$G_P^{q,N} = -4m_N^2\left(\frac{a_{q,\pi}^N}{q^2 - m_\pi^2} + \frac{a_{q,\eta}^N}{q^2 - m_\eta^2}\right), \quad (12b)$$

where

$$a^p_{u,\pi} = -a^p_{d,\pi} = \frac{1}{2} g^3_A,$$
$$a^N_{s,\pi} = 0,$$
$$a^N_{u,\eta} = a^N_{d,\eta} = -\frac{1}{2} a^N_{s,\eta} = \frac{1}{6} g^8_A,$$

with

$$g^3_A = \Delta^p_u - \Delta^p_d,$$
$$g^8_A = \Delta^p_u + \Delta^p_d - 2\Delta^p_s.$$

Isospin symmetry implies $a^p_{u,\pi} = a^n_{d,\pi}$ and $a^p_{d,\pi} = a^n_{u,\pi}$. We use the values $\Delta^p_u = \Delta^n_d = 0.842$, $\Delta^p_d = \Delta^n_u = -0.427$, $\Delta^N_s = -0.085$ [90] and neglect further dependencies on momentum transfer.

In the case of nuclei $\mathcal{N}$ instead of a nucleon, we express the nuclear matrix elements in the same way as in Eqs. (9) with nuclear form factors $F_i^{f,\mathcal{N}}(q^2)$, $G_i^{f,\mathcal{N}}(q^2)$, i.e.,

$$\langle \mathcal{N}(p')|\bar{f}\gamma^\mu f|\mathcal{N}(p)\rangle = \bar{u}(p')\left[F_1^{f,\mathcal{N}}(q^2)\gamma^\mu + F_2^{f,\mathcal{N}}(q^2)\frac{i\sigma^{\mu\nu}q_\nu}{2m_\mathcal{N}}\right]u(p), \quad (13a)$$

$$\langle \mathcal{N}(p')|\bar{f}\gamma^\mu\gamma^5 f|\mathcal{N}(p)\rangle = \bar{u}(p')\left[G_A^{f,\mathcal{N}}(q^2)\gamma^\mu\gamma^5 + G_P^{f,\mathcal{N}}(q^2)\frac{\gamma^5 q^\mu}{2m_\mathcal{N}}\right]u(p). \quad (13b)$$

For simplicity, in this work we consider the $q^2 = 0$ approximation of the form factors and nuclear matrix elements of nuclei, namely $F_i^{f,\mathcal{N}}$, are obtained from up- and down-quark form factors in the same way as for the nucleons in Eq. (10). As we show below, the effect of axial couplings is strongly suppressed in the parity asymmetry parameter and nuclear weak charge. Therefore, in summary, we only use the F_1 form factors when considering nuclei ^{12}C and ^{133}Cs, which gives the dominating contribution.

B. Asymmetry parameter

Concentrating on the electron-nucleus cross section induced by $\mathcal{L}_{\rm PV}$ in Eq. (2) together with SM physics, i.e., photon and Z boson exchange, we note that the amplitudes for left-handed or right-handed incoming electrons can be written as

$$i\mathcal{M}^{\pm s' r r'}_{L,R} = \sum_{j=1}^{8}\frac{K_j}{\Lambda^2}(\bar{u}_{s'}(k_e)\mathcal{O}_j u_\pm(p_e)) \times (\bar{u}_{r'}(k_\mathcal{N})\mathcal{O}_j{}' u_r(p_\mathcal{N})). \quad (14)$$

where K_j, $\mathcal{O}_j$, and $\mathcal{O}_j{}'$ are given in Table II for the general case. In this calculation we equate helicity and chirality of the incoming electron in order to replace $u_\pm(p_e)$ by $P_{R/L}u_s(p_e)$ and using trace identities from summing over s. The correction to the amplitude due to this approximation should be of order $m_e/|p_e| \approx 0.5$ MeV$/155$ MeV$\approx 3\times10^{-3}$ and is negligible for our purposes.

TABLE II. Coefficients appearing in the amplitude of chiral electron-proton scattering Eq. (17).

j	K_j	$\mathcal{O}_j$	$\mathcal{O}'_j$
1	$C_{LVu}F_1^{u,\mathcal{N}} + C_{LVd}F_1^{d,\mathcal{N}}$	$\gamma_\mu P_L$	γ^μ
2	$C_{LVu}F_2^{u,\mathcal{N}} + C_{LVd}F_2^{d,\mathcal{N}}$	$\gamma_\mu P_L$	$i\sigma^{\mu\nu}q_\nu/2m\mathcal{N}$
3	$C_{RVu}F_1^{u,\mathcal{N}} + C_{RVd}F_1^{d,\mathcal{N}}$	$\gamma_\mu P_R$	γ^μ
4	$C_{RVu}F_2^{u,\mathcal{N}} + C_{RVd}F_2^{d,\mathcal{N}}$	$\gamma_\mu P_R$	$i\sigma^{\mu\nu}q_\nu/2m\mathcal{N}$
5	$C_{LAu}G_A^{u,\mathcal{N}} + C_{LAd}G_A^{d,\mathcal{N}}$	$\gamma_\mu P_L$	$\gamma^\mu\gamma^5$
6	$C_{LAu}G_P^{u,\mathcal{N}} + C_{LAd}G_P^{d,\mathcal{N}}$	$\gamma_\mu P_L$	$\gamma^5 q^\mu/2m_\mathcal{N}$
7	$C_{RAu}G_A^{u,\mathcal{N}} + C_{RAd}G_A^{d,\mathcal{N}}$	$\gamma_\mu P_R$	$\gamma^\mu\gamma^5$
8	$C_{RAu}G_P^{u,\mathcal{N}} + C_{RAd}G_P^{d,\mathcal{N}}$	$\gamma_\mu P_R$	$\gamma^5 q^\mu/2m_\mathcal{N}$

The differential cross section for initial polarization X is proportional to the squared matrix element,

$$\frac{d\sigma_X}{dt} \sim |\mathcal{M}_X|^2, \quad (15)$$

(t being the Mandelstam variable) and therefore the asymmetry parameter is simply given by the squared amplitudes in the form of

$$A_{\rm PV} = \frac{\frac{d\sigma_R}{dt} - \frac{d\sigma_L}{dt}}{\frac{d\sigma_R}{dt} + \frac{d\sigma_L}{d0}} = \frac{|\mathcal{M}_R|^2 - |\mathcal{M}_L|^2}{|\mathcal{M}_R|^2 + |\mathcal{M}_L|^2}, \quad (16)$$

where

$$|\mathcal{M}_{L,R}|^2 = \frac{1}{2}\sum_{j=1}^{8}\sum_{k=1}^{8}\frac{1}{\Lambda^4}K_j K_k^* \sum_{s,s',r,r'=\pm}\mathrm{tr}[(\not{k}_e + m_e)\mathcal{O}_j P_{L,R}(\not{p}_e + m_e)P_{R,L}\gamma^0\mathcal{O}_k^\dagger\gamma^0]\mathrm{tr}[(\not{k}_\mathcal{N} + m_\mathcal{N})\mathcal{O}'_j(\not{p}_\mathcal{N} + m_\mathcal{N})\gamma^0\mathcal{O}'^\dagger_k\gamma^0]. \quad (17)$$

To account also for the SM contributions of photon and Z boson exchange in the calculation we replace in Table II

$$\frac{C_{XVf}}{\Lambda^2} \to \frac{-4\pi\alpha q_f}{q^2} + \frac{g^2}{2c_W^2}\frac{g_X^e g_V^f}{q^2 - m_Z^2} + \frac{C_{XVf}}{\Lambda^2}, \quad (18a)$$

$$\frac{C_{XAf}}{\Lambda^2} \to \frac{g^2}{2c_W^2}\frac{g_X^e g_A^f}{q^2 - m_Z^2} + \frac{C_{XAf}}{\Lambda^2}, \tag{18b}$$

where the SM charges and couplings are, as usual, $g^2 = 4\pi\alpha/s_W^2$ (with $s_W \equiv \sin\theta_W$ being the sine of the weak mixing angle, and $\alpha = e^2/4\pi$ being the fine-structure constant), and

$$\begin{aligned} q_u &= \frac{2}{3}, \qquad q_d = -\frac{1}{3}, \\ g_V^u &= \frac{1}{2} - \frac{4}{3}s_W^2, \qquad g_A^u = \frac{1}{2}, \\ g_V^d &= -\frac{1}{2} + \frac{2}{3}s_W^2, \qquad g_A^d = -\frac{1}{2}, \\ g_L^e &= -\frac{1}{2} + s_W^2, \qquad g_R^e = s_W^2. \end{aligned} \tag{19}$$

The full resulting expression is too lengthy to reproduce here. It is, however, illustrative to rederive certain limits from it. To recover the leading-order SM expectation for the case of a proton, we can set all C coefficients to zero such that the term of leading order in q^2/m_Z^2 reads

$$A_{\rm PV}^{\rm LO} = \frac{g^2}{2c_W^2}\frac{(g_R^e - g_L^e)(F_1^{u,p}(q^2)g_V^u + F_1^{d,p}(q^2)g_V^d)}{4\pi\alpha(F_1^{u,p}q_u + F_1^{d,p}q_d)}\frac{q^2}{m_Z^2}. \tag{20}$$

Taking $F_1^{u,p}(q^2) \approx F_q^{u,p}(0) = 2$ and $F_1^{d,p}(q^2) \approx F_q^{d,p}(0) = 1$ we obtain the standard result [70]

$$A_{\rm PV}^{\rm LO} = \frac{g^2}{2c_W^2}\frac{(g_R^e - g_L^e)(2g_V^u + g_V^d)}{4\pi\alpha(4/3 - 1/3)} = -\frac{G_F}{\sqrt{2}}\frac{Q^2}{4\pi\alpha}(1 - 4s_W^2), \tag{21}$$

where $Q^2 \equiv -q^2$. We observe that (weak) axial charges do not contribute at leading order in the proton case. Evaluating this expression at the central value for the scattering angle in P2, $q^2 = -(93\ \text{MeV})^2$, and for the expected low-energy value of the Weinberg angle, $s_W^2 = 0.23$, results in $A_{\rm PV}^{\rm LO} = -4.815 \times 10^{-8}$ for the proton. This deviates from the SM expectation $A_{\rm PV}^{\rm pred} = -3.994 \times 10^{-8}$ due to radiative corrections [70]. Instead of accounting for all corrections, we will consider the relative strength of deviations from the expected asymmetry due to new physics contributions $A_{\rm PV}^{\rm NP}$, that is, we consider $\Delta A_{\rm PV}^{\rm NP}/A_{\rm PV}^{\rm pred}$ as detailed below. Before doing that, we state the leading-order asymmetry in the case of ^{12}C. In this case we have, approximately, $F_1^{u,^{12}\rm C} \approx 6n_{u,p} + 6n_{u,n} = 18$ and $F_1^{d,^{12}\rm C} \approx 6n_{d,p} + 6n_{d,n} = 18$, where $n_{f,N}$ denotes the number of valence quarks f contained in the nucleon N, such that

$$A_{\rm PV}^{\rm LO} = \frac{g^2}{2c_W^2}\frac{(g_R^e - g_L^e)(18g_V^u + 18g_V^d)}{4\pi\alpha 18(2/3 - 1/3)} = \frac{G_F}{\sqrt{2}}\frac{Q^2}{4\pi\alpha}4s_W^2. \tag{22}$$

We have examined possible uncertainties on the theoretical predictions for $A_{\rm PV}$ and identified that the largest uncertainty arises from the form factors. The various form factors used in the calculation are generally q^2 dependent. The weak interaction contribution relies on the weak charge form factor

$$F_Z(q^2) = F_1^{u,p}(q^2)g_V^u + F_1^{d,p}(q^2)g_V^d \tag{23}$$

(for leptoquark and other new physics, one has different combinations of $F_1^{u,p}$ and $F_1^{d,p}$) which differs from the electric charge form factor

$$F_\gamma(q^2) = F_1^{u,p}(q^2)q_u + F_1^{d,p}(q^2)q_d. \tag{24}$$

When q^2 is not negligibly small, the q^2 dependence of these form factors corrects the results as

$$A_{\rm PV} \to A_{\rm PV}\frac{F_Z(q^2)}{F_Z(0)}\frac{F_\gamma(0)}{F_\gamma(q^2)}. \tag{25}$$

A simple approach to estimate the correction is to make use of

$$R_{Z/\gamma}^2 \equiv \frac{6}{F_{Z/\gamma}(0)}\left.\frac{dF_{Z/\gamma}(q^2)}{dq^2}\right|_{q^2\to 0},$$

which is the weak/electric charge radius of proton. Using experimentally determined values $R_\gamma \approx 0.84$ fm and $R_Z \approx 1.55$ fm [91], we obtain $F_\gamma(q^2)/F_\gamma(0) \approx 1 - 0.026$ and $F_Z(q^2)/F_Z(0) \approx 1 - 0.089$ for $q^2 = -(93\ \text{MeV})^2$, and hence $A_{\rm PV} \to (1 - 0.063)A_{\rm PV}$, which implies that including the q^2 dependence of form factors leads to a 6.3% smaller value of $A_{\rm PV}$ in the SM. As for new physics predictions, the results generally depend on different combinations of $F_1^{u,p}(q^2)$ and $F_1^{d,p}(q^2)$, and hence different form factors. The uncertainty according to the above analysis is expected to be at the percent level as well. For ^{12}C, the correction is also at the percent level according to the Helm analytic approximation for nuclear form factors [92].

C. SMEFT operators

Let us now consider single-operator extensions of the SM. We have to carefully expand the contributions in terms of small parameters in order to extract the correct leading contribution of a given operator. We can broadly classify the energy scales involved into small scales, m_e, m_p, E_e, q^2, and large scales m_Z and Λ. Without new physics, the results can generally be expanded in inverse powers of m_Z. In the presence of new physics parametrized by C/Λ^2, we can make a double expansion in powers m_Z^{-2n} and Λ^{-2n}. The

leading new-physics contribution, if present, should be of order Λ^{-2}. We find the following leading new-physics contributions

$$\Delta A_{\rm PV}^{LVf}(\mathcal{N}) \approx \frac{C_{LVf}}{\Lambda^2}\frac{q^2}{4\pi\alpha}\frac{F_1^{f,\mathcal{N}}}{q_u F_1^{u,\mathcal{N}} + q_d F_1^{d,\mathcal{N}}}, \tag{26a}$$

$$\Delta A_{\rm PV}^{RVf}(\mathcal{N}) \approx -\frac{C_{RVf}}{\Lambda^2}\frac{q^2}{4\pi\alpha}\frac{F_1^{f,\mathcal{N}}}{q_u F_1^{u,\mathcal{N}} + q_d F_1^{d,\mathcal{N}}}, \tag{26b}$$

$$\Delta A_{\rm PV}^{LAf}(\mathcal{N}) \approx \frac{C_{LAf}}{\Lambda^2} G_A^{f,\mathcal{N}} \frac{E_e q^4}{4\pi\alpha(2E_e^2 - m_e^2)m_{\mathcal{N}}} \times \frac{q_u(F_1^{u,\mathcal{N}} + F_2^{u,\mathcal{N}}) + q_d(F_1^{d,\mathcal{N}} + F_2^{d,\mathcal{N}})}{(q_u F_1^{u,\mathcal{N}} + q_d F_1^{d,\mathcal{N}})^2}, \tag{26c}$$

$$\Delta A_{\rm PV}^{RAf}(\mathcal{N}) \approx \frac{C_{RAf}}{\Lambda^2} G_A^{f,\mathcal{N}} \frac{E_e q^4}{4\pi\alpha(2E_e^2 - m_e^2)m_{\mathcal{N}}} \times \frac{q_u(F_1^{u,\mathcal{N}} + F_2^{u,\mathcal{N}}) + q_d(F_1^{d,\mathcal{N}} + F_2^{d,\mathcal{N}})}{(q_u F_1^{u,\mathcal{N}} + q_d F_1^{d,\mathcal{N}})^2}, \tag{26d}$$

where $f = u, d$. This also shows that the sensitivity on axial interactions is lower due to the additional suppression by $q^2/(m_{\mathcal{N}} E_e)$. One can check numerically for proton and ^{12}C that these are indeed the leading contributions to the correction to the asymmetry. However, we will use the exact expressions for our numerical results. It is not surprising that no power of m_Z^{-2} is required here, because these four operators are by themselves parity-violating. The (pseudo)scalar and tensor operators, being parity-conserving, would require a cross-term with the SM-intrinsic parity violation expressed through the Z-couplings in order to contribute to $\Delta A_{\rm PV}$. Therefore the sensitivity of P2 to those interactions is very weak. This justifies again our separation into parity-violating interactions in Eq. (2) and parity-conserving interactions in Eq. (4).

The sensitivity of P2 to new physics can be estimated by the same method as in Ref. [71]. Namely, we require that the new physics contribution does not exceed

$$\frac{\Delta A_{\rm PV}}{A_{\rm PV}} = \begin{cases} \sqrt{3.84} \times 1.4\% = 2.74\% & \mathcal{N} = p, \\ \sqrt{3.84} \times 0.3\% = 0.59\% & \mathcal{N} = {}^{12}\mathrm{C}, \end{cases} \tag{27}$$

which corresponds to 95% CL. These numbers correspond to the expected sensitivities of the P2 experiment according to Ref. [70]. For the normalization in the case of protons, we use the expected SM value $A_{\rm PV}^{\rm pred} = -3.994 \times 10^{-8}$. For the normalization in the case of ^{12}C, we use the leading-order SM result from our own calculation. Moreover, we approximate $F_1^{u,^{12}\mathrm{C}} = F_1^{d,^{12}\mathrm{C}} = 18$ while neglecting the other form factors. This leads to expected minimal values for new physics scales $\Lambda/\sqrt{C}$ given in Table III. If we use the replacement rules Eq. (3), we can alternatively project bounds on SMEFT coefficients in the same way. The results are collected in Table IV along with existing bounds from APV and ATLAS dilepton searches discussed in Sec. IV.

TABLE III. Expected bounds at 95% CL on the scale $\Lambda/\sqrt{C}$ of the operators in Eq. (3a) from P2 for the case of proton and carbon targets, assuming a single coupling at a time.

Target	C	$\Lambda/\sqrt{C}$ (TeV)	C	$\Lambda/\sqrt{C}$ (TeV)
p	C_{LVu}	13.1	C_{LVd}	9.3
	C_{RVu}	13.1	C_{LVd}	9.3
	C_{LAu}	2.6	C_{LAd}	1.8
	C_{RAu}	2.6	C_{LAd}	1.8
^{12}C	C_{LVu}	8.4	C_{LVd}	8.4
	C_{RVu}	8.4	C_{RVd}	8.4

Here we would like to compare our results with a recent analysis in Ref. [85] which gives P2 bounds in terms of the operators $\frac{G_F}{\sqrt{2}} C_{1q}^e \bar{q}\gamma^\mu q \bar{e}\gamma_\mu\gamma_5 e$. The 2σ widths of C_{1u}^e and C_{1d}^e from Figs. 1–3 in Ref. [85] are 6.46×10^{-4} and 1.33×10^{-3} respectively. Recasting to our C_{XVu} and C_{XVd} ($X = L$ or R) Wilson coefficients, they correspond to $\Lambda/\sqrt{C} =$ 13.7 TeV and 9.6 TeV, which are consistent with the first two rows in Tab. III. Note that Ref. [85] did not consider axial-vector operators nor the ^{12}C case.

D. Leptoquarks

As obvious from Eqs. (6a)–(6g), the same SMEFT operator is generated by different leptoquarks. If we assume one coupling to dominate, we can constrain $m_{\rm LQ}/g_{\rm LQ}$ in the EFT-like limit of $m_{\rm LQ} \gg q^2$. To achieve this, one can take the expression for the asymmetry in terms of the coefficients in Eq. (3) and then use the matching of leptoquark

TABLE IV. Expected bounds at 95% CL on the scale $\Lambda/\sqrt{C}$ of SMEFT operators from P2 for the case of proton and carbon targets, assuming a single coupling at a time. These are compared to bounds from APV [72] in Sec. IV A and ATLAS dilepton limits [75] in Sec. IV B.

	$\Lambda/\sqrt{C}$ (TeV)			
Coupling	P2 (p)	P2 (^{12}C)	APV (^{133}Cs)	ATLAS dilepton
$C_{lq(1)}$	11.4	8.4	11.1	7.7
$C_{lq(3)}$	6.9	…	2.6	9.2
C_{eu}	9.4	5.9	3.2	7.5
C_{ed}	6.4	5.9	3.4	4.8
C_{qe}	11.3	8.4	4.6	7.2
C_{lu}	9.0	5.9	7.6	6.2
C_{ld}	6.7	5.9	8.1	5.0

TABLE V. Expected bounds on leptoquarks masses at 95% CL for single couplings $g_{\mathrm{LQ}} = 1$ from P2 compared with existing bounds from APV [72] and ATLAS dilepton data [75]. Additional bounds are shown in Figs. 1 and 2.

		m_{LQ}(TeV)			
Leptoquark	Coupling	P2 (p)	P2 (^{12}C)	APV (^{133}Cs)	ATLAS dilepton
S_1	s_{1L}	6.6	4.2	2.2	2.3
S_1	s_{1R}	6.6	4.2	5.4	2.6
$\tilde{S}_1$	$\tilde{s}_1$	4.5	4.2	5.7	3.1
S_3	s_3	9.2	7.3	4.0	5.0
V_2	v_{2R}	11.3	8.4	4.6	8.7
V_2	v_{2L}	6.7	5.9	8.1	6.5
$\tilde{V}_2$	$\tilde{v}_2$	9.0	5.9	7.6	7.8
R_2	r_{2R}	7.9	5.9	3.3	4.5
R_2	r_{2L}	6.4	4.2	5.4	4.1
$\tilde{R}_2$	$\tilde{r}_2$	4.7	4.2	5.7	2.3
U_1	u_{1L}	6.4	5.9	3.4	4.1
U_1	u_{1R}	6.4	5.9	8.1	4.6
$\tilde{U}_1$	$\tilde{u}_1$	9.4	5.9	7.6	7.3
U_3	u_3	14.8	10.3	5.6	10.8

couplings to SMEFT operators in Eqs. (6a)–(6g). The results are shown in Table V as well as Figs. 1–2. Since for ^{12}C we are neglecting momentum dependence of the form factors as well as the contributions of leptoquarks to axial currents [which are suppressed, as discussed below Eq. (26d)], those numbers represent the leading order with respect to form factor and momentum-dependent corrections. They are, however, sufficient to compare sensitivities of different targets to different interactions.

We observe that generically the bounds using the proton target are stronger than the ones using ^{12}C. This can be explained by the smaller $A_{\mathrm{PV}}^{\mathrm{LO}}$ of the proton, which is proportional to $(1-4s_W^2) \approx 0.08$ compared to $(4s_W^2) \approx 0.92$ for ^{12}C. Considering that ΔA_{PV} in Eqs. (26a) and (26b) for up quarks and down quarks differs only by the factors

$$\frac{F_1^{f,p}}{q_u F_1^{u,p} + q_d F_1^{d,p}} \approx \begin{cases} 2 & f = u \\ 1 & f = d \end{cases}, \tag{28a}$$

$$\frac{F_1^{f,^{12}\mathrm{C}}}{q_u F_1^{u,^{12}\mathrm{C}} + q_d F_1^{d,^{12}\mathrm{C}}} \approx \begin{cases} 3 & f = u \\ 3 & f = d \end{cases}, \tag{28b}$$

and using the expected sensitivities in Eq. (27), we can estimate that the constraints on C/Λ^2 from p should be stronger by a factor of approximately

$$\frac{0.92 \cdot 0.3\%}{0.08 \cdot 1.4\%} \cdot \begin{cases} \frac{2}{3} & f = u \\ \frac{1}{3} & f = d \end{cases} \approx \begin{cases} 1.7 & f = u \\ 0.8 & f = d \end{cases} \tag{29}$$

compared to ^{12}C. This explains why couplings to down quarks are constrained to similar magnitude, while couplings to up quarks are better constrained by proton targets. These factors, however, are not exact, since we did not take radiative and form factor corrections into account.

IV. OTHER OBSERVABLES

A number of different observables are suitable to constrain the relevant SMEFT operators or leptoquarks. Besides electron scattering, APV probes the same couplings. Additionally, we include bounds from the LHC on leptoquark production, as well as their contribution to Drell-Yan production of electron pairs. The operators involving lepton doublets can further be probed by coherent elastic neutrino-nucleus scattering (CEνNS), since they lead to analogous interactions of neutrinos with nuclei. However, currently CEνNS is not competitive with other constraints in this respect [85]. The current order of magnitude can be estimated by noting that the best constraints on neutrino nonstandard interactions (NSI) from CEνNS are at the order of $\epsilon_V \lesssim 0.5$ for vector interactions, while bounds on axial interactions are weaker [93,94]. Using the mapping between NSI and SMEFT operators, e.g., in Ref. [95], this can be translated to EFT scales of

$$\frac{\Lambda}{\sqrt{C}} \lesssim \left(\frac{G_F \epsilon_V}{\sqrt{2}}\right)^{-1/2} \approx 0.5 \text{ TeV}, \tag{30}$$

which are well below the values in Table IV. Therefore, we focus on the constraints which are most competitive with P2, namely those from APV and the LHC.

A. Atomic parity violation

As in Ref. [71], we use the most precise measurement of APV which concerns the $6S_{1/2} - 7S_{1/2}$ nuclear transition in ^{133}Cs. Following Ref. [70], we define the proton weak charge $Q_W(p)$ as the limit of the asymmetry at zero-momentum transfer, normalized such that the asymmetry formula (recall that $Q^2 = -q^2$)

$$A_{\mathrm{PV}}^{\mathrm{LO}} = -\frac{G_F}{\sqrt{2}} \frac{Q^2}{4\pi\alpha} Q_W(p) = \frac{G_F}{\sqrt{2}} \frac{q^2}{4\pi\alpha} Q_W(p) \tag{31}$$

holds, for which one can find from Eq. (21) that at leading-order the weak charge reads

$$Q_W(p) = 1 - 4s_W^2. \tag{32}$$

Generalizing to nuclei, we simplify Eq. (20) to the form

$$A_{\mathrm{PV}}^{\mathrm{LO}} = \frac{G_F}{\sqrt{2}} \frac{q^2}{4\pi\alpha} \frac{Q_W(\mathcal{N})}{F_1^{u,\mathcal{N}} q_u + F_1^{d,\mathcal{N}} q_d} \tag{33}$$

with

$$Q_W(\mathcal{N}) = 2(F_1^{u,\mathcal{N}} g_V^u + F_1^{d,\mathcal{N}} g_V^d) \approx Z(\mathcal{N})(1-4s_W^2) - N(\mathcal{N}), \tag{34}$$

where Z and N denote the nuclear charge and number of neutrons, see also Ref. [96], such that

$$Q_W(^{12}\mathrm{C}) \approx -24 s_W^2, \tag{35a}$$

$$Q_W(^{133}\mathrm{Cs}) \approx -23 - 220 s_W^2 \approx -73.6 \tag{35b}$$

consistent with Eq. (22). For ^{133}Cs, which has the currently best-measured asymmetry, we have used $Z_{\mathrm{Cs}} = 55$ and $N_{\mathrm{Cs}} = 78$. The SM prediction including radiative corrections and the measured values are given by [72]

$$Q_W^{\mathrm{SM}}(^{133}\mathrm{Cs}) = -73.23(1), \tag{36a}$$

$$Q_W^{\mathrm{exp}}(^{133}\mathrm{Cs}) = -73.71(35). \tag{36b}$$

These two numbers are consistent within 2σ. We will use them nevertheless to illustrate how P2 could confirm or resolve the mild tension [72] between theory and experiment. From Eqs. (26a)–(26d) we can see how the measured value would be changed from the SM prediction through additional contributions to interactions at quark level at leading order. Note that therefore P2 data can be used to further investigate this deviation. We do so in Sec. V, finding that P2 should be able to rule out the necessary quark-level couplings at 95% CL. We can write, for generic modifications ΔQ_W^{NP} of the weak charge,

$$A_{\mathrm{PV}} = A_{\mathrm{PV}}^{\mathrm{SM}} + \Delta A_{\mathrm{PV}}^{\mathrm{NP}} = \frac{G_F}{\sqrt{2}} \frac{q^2}{4\pi\alpha} \frac{Q_W^{\mathrm{SM}}(\mathcal{N}) + \Delta Q_W^{\mathrm{NP}}(\mathcal{N})}{F_1^{u,\mathcal{N}} q_u + F_1^{d,\mathcal{N}} q_d}, \tag{37}$$

with

$$\Delta Q_W^{\mathrm{NP}}(\mathcal{N}) = \Delta A_{\mathrm{PV}}^{\mathrm{NP}} \left(\frac{\sqrt{2}}{G_F} \frac{4\pi\alpha}{q^2} (F_1^{u,\mathcal{N}} q_u + F_1^{d,\mathcal{N}} q_d) \right).$$

In the limit $q^2 \to 0$ we conclude that, in the EFT picture,

$$\Delta Q_W^{\mathrm{NP}}(^{133}\mathrm{Cs}) = \frac{\sqrt{2}}{G_F} \frac{1}{\Lambda^2} (F_1^{u,^{133}\mathrm{Cs}} (C_{LVu} - C_{RVu}) + F_1^{d,^{133}\mathrm{Cs}} (C_{LVd} - C_{RVd})). \tag{38}$$

The momentum transfer in APV experiments is not exactly vanishing, but instead of the order of the inverse nuclear radius $Q \sim 1/r_0 \sim 30$ MeV according to Refs. [97,98]. Other references set the momentum transfer at $Q \sim 2.4$ MeV which we will adapt here when considering leptoquark propagators [82]. However, even with such nonvanishing Q the axial couplings will be poorly probed, since they contribute to ΔQ_W^{NP} only with a suppression factor of $Q/m_{\mathcal{N}} \sim 10^{-5}$. To recast the bounds on Q_W into 95% CL bounds on new physics, we will hence require that $Q_W^{\mathrm{SM}}(^{133}\mathrm{Cs}) + \Delta Q_W^{\mathrm{NP}}(^{133}\mathrm{Cs})$ does not deviate from Q_W^{exp} by more than $\sqrt{3.84}$ standard deviations, neglecting the error of the SM prediction.

The results are included in Figs. 1–2. It is interesting to note that we can identify two cases: Some leptoquarks increase Q_W while others decrease it. Now since the SM expectation is already *above* the measured value, there is less room for new physics increasing Q_W and more room for new physics decreasing Q_W. Therefore, the general pattern is that P2 is expected to improve bounds on couplings decreasing Q_W while bounds on couplings increasing Q_W will likely remain better tested by APV.

B. Collider searches

Effective interactions between two quarks and two electrons as parametrized by the SMEFT operators of Eq. (A2) and as induced, for instance, by heavy leptoquarks according to the matching in Eqs. (6a)–(6g) can be tested at the LHC by searching for deviations from the SM in the Drell-Yan (DY) process $pp \to e^+e^-$. In the case of leptoquarks, this is mediated by a t-channel exchange of a leptoquark annihilating a quark-antiquark pair and producing an electron-positron pair. The latest results from the ATLAS experiment [75][2] are given in terms of limits on the contribution of new physics to the cross section in the signal region for the cases of constructive and destructive interference. To quantify constraints implied by these limits, we simulate the expected new-physics contributions to the cross section in the signal regions of invariant masses of the dilepton system [2200, 6000] GeV (constructive interference) and [2770, 6000] GeV (destructive interference) using MADGRAPH5 [100]. As further cuts we apply $p_T > 30$ GeV and $|\eta| < 2.47$ on the final state leptons, to approximate the ATLAS specifications. We use the same parton distribution function as specified in the ATLAS analysis, namely NNPDF23LO with the LHAPDF identifier 247000. To create UFO model files, we use FEYNRULES [101,102] to extend the included SM model file by leptoquarks, or, to simulate SMEFT operators, by a heavy neutral vector boson with the appropriate couplings to match the considered Wilson coefficients.

The resulting lower bounds on the new-physics scale Λ from SMEFT operators with unit Wilson coefficients consistent with the ATLAS search are given in Table IV. Similarly, the limits on leptoquark masses calculated for single unit Yukawa couplings are given in Table V and

[2]The corresponding CMS limits [99] are weaker, so we only consider the ATLAS results.

shown in Figs. 1 and 2. We find that all couplings are currently constrained by the constructive interference bounds. As a consistency check of our results, we can compare the limit on the NP scale Λ with ATLAS results. Since they assume equal couplings to up and down quarks, we can directly compare the operator $\mathcal{O}_{qe}$ which corresponds to the scenario $\eta_{LR} = 1$ referring to the effective Lagrangian in Eq. (1) of Ref. [75]. This operator is also induced by the r_{2R} leptoquark coupling. Therefore we can map both our EFT limit and our leptoquark limit to constraints on the scale Λ_{ATLAS} used in Ref. [75] in the following way:

$$\frac{4\pi}{\Lambda^2_{\mathrm{ATLAS}}} = \frac{|r_{2R}|^2}{2m^2_{R_2}}$$
$$\Rightarrow \Lambda_{\mathrm{ATLAS}} \geq \sqrt{8\pi} m_{R_2} = 22.6 \text{ TeV}, \tag{39a}$$

$$\frac{4\pi}{\Lambda^2_{\mathrm{ATLAS}}} = \frac{C_{qe}}{\Lambda^2}$$
$$\Rightarrow \Lambda_{\mathrm{ATLAS}} \geq \sqrt{4\pi}\frac{\Lambda}{\sqrt{C_{qe}}} = 25.5 \text{ TeV}. \tag{39b}$$

Comparing to the ATLAS result of $\Lambda_{\mathrm{ATLAS}} \geq 24.7$ TeV we conclude that our method produces reasonable results. These results are also comparable to those obtained in Ref. [85].

The presence of leptoquarks can also be tested at proton colliders through pair production or single resonant production (SRP). While pair production through gluon fusion dominates for small Yukawa couplings $g_{\mathrm{LQ}} \lesssim 0.1$–$1$ since its cross section is determined by the strong gauge coupling, SRP can be relevant for larger couplings [76]. In Figs. 1 and 2 we show bounds from SRP calculated in Ref. [76]. Turning to pair production, in our cases for single leptoquark couplings to electrons and first-generation quarks, the resulting signal from the subsequent decays of the leptoquark pair is given by an $e^+ - e^-$-pair and two jets. Assuming the lifetime of leptoquarks is short enough, this search yields a lower bound on the leptoquark mass. In Ref. [73] the search is done for scalar leptoquarks giving a lower limit on the mass of about 1.8 TeV at 95% CL for leptoquarks coupling to singlets. Following the prescription of Ref. [74], we rescale these limits by scaling the pair production cross sections of different leptoquarks depending on their coupling types and comparing them to the exclusion curve of Ref. [73]. The resulting bounds are included in Figs. 1 and 2.

V. POTENTIAL TO RESOLVE DEGENERACIES USING MULTIPLE TARGETS

In Fig. 3, we show for two SMEFT coefficients at a time how the different measurements constrain the combination of parameters and break degeneracies single measurements suffer from. While the seven parity-violating Wilson coefficients appearing in Eq. (3) can be combined in 21 different ways, we only show some of the combinations, since many are basically equivalent. This is because the effective contribution to the asymmetry parameter for protons and nuclei is mainly controlled by the two effective up quark and down quark coupling coefficients

$$C_{\mathrm{PV}u} = C_{LVu} - C_{RVu} = \frac{1}{2}(C_{lq(1)} - C_{lq(3)} - C_{qe} - C_{eu} + C_{lu}), \tag{40a}$$

$$C_{\mathrm{PV}d} = C_{LVd} - C_{RVd} = \frac{1}{2}(C_{lq(1)} + C_{lq(3)} - C_{qe} - C_{ed} + C_{ld}), \tag{40b}$$

as one can see by adding up $\Delta A^{LVf}_{\mathrm{PV}}(\mathcal{N})$ and $\Delta A^{RVf}_{\mathrm{PV}}(\mathcal{N})$ in Eqs. (26a)–(26b) for up and down quarks, respectively. From this we can group coefficients into smaller sets which have a nondistinguishable effect. Namely,

(i) $C_{lq(1)}$ and C_{qe} have the same effect (equal contribution to up and down couplings) with opposite sign.
(ii) C_{eu} and C_{lu} have the same effect (contribution only to up couplings) with opposite sign.
(iii) C_{ed} and C_{ld} have the same effect (contribution only to down couplings) with opposite sign.
(iv) $C_{lq(3)}$ forms its own group (contribution to up and down couplings with same magnitude but opposite sign).

Therefore, we plot only one example of each of these groups in comparison in Fig. 3. We find that the comparison of nuclei with protons is particularly good at resolving degeneracies between $C_{lq(3)}$ and other operators. However, the comparison between p and ^{12}C can also be expected to distinguish well between up quark and down quark interactions, as seen in the plot of C_{eu} against C_{ed}. Moreover, if the SM expectation marked by an asterisk turns out to be correct [see the discussion after Eq. (36a)], we can see that the current best fit of APV, shown as dark green lines, can be expected to be ruled out by combining proton and ^{12}C measurements of P2.

VI. CONCLUSION

In our study of the potential of the P2 experiment to test parity-violating new physics induced by SMEFT operators or leptoquarks, we found that P2 can be expected to be competitive with existing collider searches for such new physics and in many cases to have a better sensitivity to leptoquarks with masses above around 2 TeV. For all single operator scenarios and most single leptoquark scenarios, bounds from APV experiments with ^{133}Cs can be exceeded by P2. We stress, however, that the complementarity of using different targets, for instance protons and ^{12}C at P2, as

well as ^{133}Cs in APV will allow to better disentangle up and down quark interactions as illustrated in Fig. 3. Moreover, a potential tension between theoretical and experimentally determined weak charges of ^{133}Cs could be either confirmed or resolved at 95% CL by P2 data.

ACKNOWLEDGMENTS

We thank Sudip Jana for helpful discussions. I. B. acknowledges support by the IMPRS-PTFS. The work of B. D. is supported in part by the U.S. Department of Energy under Grant No. DE-SC0017987. The work of Y. Z. is supported by the National Natural Science Foundation of China under Grant No. 12175039, the 2021 Jiangsu Shuangchuang (Mass Innovation and Entrepreneurship) Talent Program No. JSSCBS20210144, and the "Fundamental Research Funds for the Central Universities". X. J. X. is supported in part by the National Natural Science Foundation of China under Grant No. 12141501.

APPENDIX A: MAPPING OF SMEFT COEFFICIENTS TO THE FLAVOR BASIS

If one starts with the SMEFT operators $\mathcal{O}_{lq(1)}$, $\mathcal{O}_{lq(3)}$, $\mathcal{O}_{lu}$, $\mathcal{O}_{ld}$, $\mathcal{O}_{qe}$, $\mathcal{O}_{eu}$, $\mathcal{O}_{ed}$, $\mathcal{O}_{ledq}$, $\mathcal{O}_{lequ(1)}$, and $\mathcal{O}_{lequ(3)}$ in the flavor basis, after making the basis change

$$u'_{L\alpha} = (V^\dagger)_{\alpha\beta} u_{L\beta}, \qquad d'_{L\alpha} = d_{L\alpha}, \qquad e'_{L\alpha} = e_{L\alpha},$$
$$u'_{R\alpha} = u_{R\alpha}, \qquad d'_{R\alpha} = d_{R\alpha}, \qquad e'_{R\alpha} = e_{R\alpha}, \tag{A1}$$

with V being the CKM matrix between primed flavor basis and unprimed mass basis, one finds

$$\begin{aligned}\mathcal{L} = \frac{1}{\Lambda^2}\{&(\tilde{C}_{lq(1)} - \tilde{C}_{lq(3)})(\bar{e}\gamma_\mu P_L e)(\bar{u}\gamma^\mu P_L u) + C_{lu}(\bar{e}\gamma_\mu P_L e)(\bar{u}\gamma^\mu P_R u) + (\bar{C}_{lq(1)} + \bar{C}_{lq(3)})(\bar{e}\gamma_\mu P_L e)(\bar{d}\gamma^\mu P_L d)\\ &+ C_{ld}(\bar{e}\gamma_\mu P_L e)(\bar{d}\gamma^\mu P_R d) + C_{qe}(\bar{e}\gamma_\mu P_R e)(\bar{u}\gamma^\mu P_L u) + C_{eu}(\bar{e}\gamma_\mu P_R e)(\bar{u}\gamma^\mu P_R u) + C_{qe}(\bar{e}\gamma_\mu P_R e)(\bar{d}\gamma^\mu P_L d)\\ &+ C_{ed}(\bar{e}\gamma_\mu P_R e)(\bar{d}\gamma^\mu P_R d) - C_{lequ(1)}(\bar{e}P_R e)(\bar{u}P_R u) - C^*_{lequ(1)}(\bar{e}P_L e)(\bar{u}P_L u)\\ &+ C_{ledq}(\bar{e}P_R e)(\bar{d}P_L d) + C^*_{ledq}(\bar{e}P_L e)(\bar{d}P_R d) - C_{lequ(3)}(\bar{e}\sigma_{\mu\nu}P_R e)(\bar{u}\sigma^{\mu\nu}P_R u) - C^*_{lequ(3)}(\bar{e}\sigma_{\mu\nu}P_L e)(\bar{u}\sigma^{\mu\nu}P_L u)\}.\end{aligned} \tag{A2}$$

The Wilson coefficients in Eq. (A2) are related to the Wilson coefficients $C'^{\alpha\beta\gamma\delta}_j$ defined for flavor eigenstates by the following identities for the parity-violating operators:

$$\begin{aligned}\tilde{C}_{lq(1)} &= V_{u\gamma}V^*_{u\delta}C'^{ee\gamma\delta}_{lq(1)}, \qquad \tilde{C}_{lq(3)} = V_{u\gamma}V^*_{u\delta}C'^{ee\gamma\delta}_{lq(3)},\\ \bar{C}_{lq(1)} &= C'^{ee11}_{lq(1)}, \qquad \bar{C}_{lq(3)} = C'^{ee11}_{lq(3)},\\ C_{lu} &= C'^{ee11}_{lu}, \qquad C_{ld} = C'^{ee11}_{ld},\\ C_{eu} &= C'^{ee11}_{eu}, \qquad C_{ed} = C'^{ee11}_{ed},\\ C_{qe} &= C'^{ee11}_{qu}.\end{aligned} \tag{A3}$$

The notation of mass-basis coefficients is the same as it appears in Eq. (3a). Only two coefficients, $C_{lq(1)}$ and $C_{lq(3)}$ remain to be clarified. If we assume only first generation flavor couplings, we can set $\tilde{C}_{lq(1)} = |V_{ud}|^2 C'^{ee11}_{lq(1)}$ and $\tilde{C}_{lq(3)} = |V_{ud}|^2 C'^{ee11}_{lq(3)}$. Equating the Lagrangian of Eq. (A2) with the sum of Eq. (2) plus Eq. (4), we identify

$$\begin{aligned}C_{lq(1)} - C_{lq(3)} &= |V_{ud}|^2 (C'^{ee11}_{lq(1)} - \tilde{C}'^{ee11}_{lq(3)}),\\ C_{lq(1)} + C_{lq(3)} &= (C'^{ee11}_{lq(1)} - C'^{ee11}_{lq(3)}).\end{aligned} \tag{A4}$$

For the parity-conserving operators, we have

$$\begin{aligned}C_{lequ(1)} &= V^*_{u\gamma} C'^{ee\gamma 1}_{lequ(1)},\\ C_{lequ(3)} &= V^*_{u\gamma} C'^{ee\gamma 1}_{eluq(3)},\\ C_{ledq} &= C'^{ee11}_{ledq}.\end{aligned} \tag{A5}$$

APPENDIX B: PARAMETRIZATION OF THE FORM FACTORS

In this section, we follow the notation of Ref. [70]. The electromagnetic Sachs form factors of the proton can be parametrized by a model multiplying a dipole and a polynomial,

$$G^p_E = \left(1 - \frac{q^2}{0.71\ \text{GeV}^2}\right)^{-2}\left(1 - \sum_{i=1}^{8}\kappa_i^{E,p} q^{2i}\right), \tag{B1a}$$

$$G^p_M = \frac{\mu_\text{P}}{\mu_\text{N}}\left(1 - \frac{q^2}{0.71\ \text{GeV}^2}\right)^{-2}\left(1 - \sum_{i=1}^{8}\kappa_i^{M,p} q^{2i}\right), \tag{B1b}$$

where $\mu_\text{P} = 2.792847356\mu_\text{N}$ denotes the proton's magnetic moment and $\mu_\text{N} = (e\hbar)/(2m_p)$ denotes the nuclear magneton. The fit coefficients κ_i are given in Tables 17 and 18 of Ref. [70]. For the neutron form factors we use

$$G_E^n = \frac{\kappa_1^{E,n}\tau}{1+\kappa_2^{E,n}\tau}\left(1-\frac{q^2}{0.71\ \text{GeV}^2}\right)^{-2}, \tag{B2a}$$

$$G_M^n = \sum_{i=0}^{9}\kappa_i^{M,n}q^{2i}, \tag{B2b}$$

where $\tau = -q^2/4m_p^2$ and the coefficients being given in Tables 19 and 20 of Ref. [70]. For the strangeness form factors we use

$$G_E^s = \frac{\kappa_1^{E,s}\tau}{1+\kappa_2^{E,s}\tau}\left(1-\frac{q^2}{0.71\ \text{GeV}^2}\right)^{-2}, \tag{B3a}$$

$$G_M^s = \kappa_0^{M,s} - \kappa_1^{M,s}q^2, \tag{B3b}$$

with the coefficients taken from Tables 21 and 22 of Ref. [70].

[1] I. Doršner, S. Fajfer, A. Greljo, J. F. Kamenik, and N. Košnik, Physics of leptoquarks in precision experiments and at particle colliders, Phys. Rep. **641**, 1 (2016).
[2] J. C. Pati and A. Salam, Lepton number as the fourth color, Phys. Rev. D **10**, 275 (1974).
[3] G. Senjanovic and A. Sokorac, Light leptoquarks in SO (10), Z. Phys. C **20**, 255 (1983).
[4] H. Murayama and T. Yanagida, A viable SU(5) GUT with light leptoquark bosons, Mod. Phys. Lett. A **07**, 147 (1992).
[5] P. H. Frampton, Light leptoquarks as possible signature of strong electroweak unification, Mod. Phys. Lett. A **07**, 559 (1992).
[6] J. L. Hewett and T. G. Rizzo, Much ado about leptoquarks: A comprehensive analysis, Phys. Rev. D **56**, 5709 (1997).
[7] I. Dorsner and P. Fileviez Perez, Unification without supersymmetry: Neutrino mass, proton decay and light leptoquarks, Nucl. Phys. **B723**, 53 (2005).
[8] N. Assad, B. Fornal, and B. Grinstein, Baryon number and lepton universality violation in leptoquark and diquark models, Phys. Lett. B **777**, 324 (2018).
[9] C. Murgui and M. B. Wise, Scalar leptoquarks, baryon number violation, and Pati-Salam symmetry, Phys. Rev. D **104**, 035017 (2021).
[10] S. S. Gershtein, A. A. Likhoded, and A. I. Onishchenko, TeV-scale leptoquarks from GUTs/string/M-theory unification, Phys. Rep. **320**, 159 (1999).
[11] R. Barbier *et al.*, R-parity violating supersymmetry, Phys. Rep. **420**, 1 (2005).
[12] D. Aristizabal Sierra, M. Hirsch, and S. G. Kovalenko, Leptoquarks: Neutrino masses and accelerator phenomenology, Phys. Rev. D **77**, 055011 (2008).
[13] K. S. Babu and J. Julio, Two-loop neutrino mass generation through leptoquarks, Nucl. Phys. **B841**, 130 (2010).
[14] I. Doršner, S. Fajfer, and N. Košnik, Leptoquark mechanism of neutrino masses within the grand unification framework, Eur. Phys. J. C **77**, 417 (2017).
[15] Y. Cai, J. Herrero-García, M. A. Schmidt, A. Vicente, and R. R. Volkas, From the trees to the forest: A review of radiative neutrino mass models, Front. Phys. **5**, 63 (2017).
[16] K. S. Babu, P. S. B. Dev, S. Jana, and A. Thapa, Non-standard interactions in radiative neutrino mass models, J. High Energy Phys. 03 (2020) 006.
[17] N. G. Deshpande and A. Menon, Hints of R-parity violation in B decays into $\tau\nu$, J. High Energy Phys. 01 (2013) 025.
[18] Y. Sakaki, M. Tanaka, A. Tayduganov, and R. Watanabe, Testing leptoquark models in $\bar{B} \to D^{(*)}\tau\bar{\nu}$, Phys. Rev. D **88**, 094012 (2013).
[19] R. Alonso, B. Grinstein, and J. Martin Camalich, Lepton universality violation and lepton flavor conservation in B-meson decays, J. High Energy Phys. 10 (2015) 184.
[20] L. Calibbi, A. Crivellin, and T. Ota, Effective Field Theory Approach to $b \to s\ell\ell^{(\prime)}$, $B \to K^{(*)}\nu\bar{\nu}$ and $B \to D^{(*)}\tau\nu$ with Third Generation Couplings, Phys. Rev. Lett. **115**, 181801 (2015).
[21] M. Freytsis, Z. Ligeti, and J. T. Ruderman, Flavor models for $\bar{B} \to D^{(*)}\tau\bar{\nu}$, Phys. Rev. D **92**, 054018 (2015).
[22] M. Bauer and M. Neubert, Minimal Leptoquark Explanation for the $R_{D^{(*)}}$, R_K, and $(g-2)_\mu$ Anomalies, Phys. Rev. Lett. **116**, 141802 (2016).
[23] S. Fajfer and N. Košnik, Vector leptoquark resolution of R_K and $R_{D^{(*)}}$ puzzles, Phys. Lett. B **755**, 270 (2016).
[24] X.-Q. Li, Y.-D. Yang, and X. Zhang, Revisiting the one leptoquark solution to the $R(\mathrm{D}^{(*)})$ anomalies and its phenomenological implications, J. High Energy Phys. 08 (2016) 054.
[25] D. Bečirević, S. Fajfer, N. Košnik, and O. Sumensari, Leptoquark model to explain the B-physics anomalies, R_K and R_D, Phys. Rev. D **94**, 115021 (2016).
[26] S. Sahoo, R. Mohanta, and A. K. Giri, Explaining the R_K and $R_{D^{(*)}}$ anomalies with vector leptoquarks, Phys. Rev. D **95**, 035027 (2017).
[27] G. Hiller, D. Loose, and K. Schönwald, Leptoquark flavor patterns & B decay anomalies, J. High Energy Phys. 12 (2016) 027.
[28] B. Bhattacharya, A. Datta, J.-P. Guévin, D. London, and R. Watanabe, Simultaneous explanation of the R_K and $R_{D^{(*)}}$ puzzles: A model analysis, J. High Energy Phys. 01 (2017) 015.
[29] O. Popov and G. A. White, One leptoquark to unify them? Neutrino masses and unification in the light of $(g-2)_\mu$, $R_{D^{(*)}}$ and R_K anomalies, Nucl. Phys. **B923**, 324 (2017).
[30] R. Barbieri, C. W. Murphy, and F. Senia, B-decay anomalies in a composite leptoquark model, Eur. Phys. J. C **77**, 8 (2017).

[31] E. Coluccio Leskow, G. D'Ambrosio, A. Crivellin, and D. Müller, $(g-2)\mu$, lepton flavor violation, and Z decays with leptoquarks: Correlations and future prospects, Phys. Rev. D **95**, 055018 (2017).

[32] A. Crivellin, D. Müller, and T. Ota, Simultaneous explanation of $R(\mathrm{D}^{(*)})$ and $b \to s\mu^+\mu^-$: The last scalar leptoquarks standing, J. High Energy Phys. 09 (2017) 040.

[33] G. Hiller and I. Nisandzic, R_K and R_{K^*} beyond the standard model, Phys. Rev. D **96**, 035003 (2017).

[34] Y. Cai, J. Gargalionis, M. A. Schmidt, and R. R. Volkas, Reconsidering the one leptoquark solution: Flavor anomalies and neutrino mass, J. High Energy Phys. 10 (2017) 047.

[35] W. Altmannshofer, P. S. B. Dev, and A. Soni, $R_{D^{(*)}}$ anomaly: A possible hint for natural supersymmetry with R-parity violation, Phys. Rev. D **96**, 095010 (2017).

[36] D. Buttazzo, A. Greljo, G. Isidori, and D. Marzocca, B-physics anomalies: A guide to combined explanations, J. High Energy Phys. 11 (2017) 044.

[37] L. Di Luzio, A. Greljo, and M. Nardecchia, Gauge leptoquark as the origin of B-physics anomalies, Phys. Rev. D **96**, 115011 (2017).

[38] L. Calibbi, A. Crivellin, and T. Li, Model of vector leptoquarks in view of the B-physics anomalies, Phys. Rev. D **98**, 115002 (2018).

[39] M. Blanke and A. Crivellin, B Meson Anomalies in a Pati-Salam Model within the Randall-Sundrum Background, Phys. Rev. Lett. **121**, 011801 (2018).

[40] D. Bečirević, I. Doršner, S. Fajfer, N. Košnik, D. A. Faroughy, and O. Sumensari, Scalar leptoquarks from grand unified theories to accommodate the B-physics anomalies, Phys. Rev. D **98**, 055003 (2018).

[41] A. Crivellin, C. Greub, D. Müller, and F. Saturnino, Importance of Loop Effects in Explaining the Accumulated Evidence for New Physics in B Decays with a Vector Leptoquark, Phys. Rev. Lett. **122**, 011805 (2019).

[42] J. Heeck and D. Teresi, Pati-Salam explanations of the B-meson anomalies, J. High Energy Phys. 12 (2018) 103.

[43] A. Angelescu, D. Bečirević, D. A. Faroughy, and O. Sumensari, Closing the window on single leptoquark solutions to the B-physics anomalies, J. High Energy Phys. 10 (2018) 183.

[44] S. Iguro, T. Kitahara, Y. Omura, R. Watanabe, and K. Yamamoto, D^* polarization vs. $R_{D^{(*)}}$ anomalies in the leptoquark models, J. High Energy Phys. 02 (2019) 194.

[45] B. Chauhan and S. Mohanty, Leptoquark solution for both the flavor and ANITA anomalies, Phys. Rev. D **99**, 095018 (2019).

[46] B. Fornal, S. A. Gadam, and B. Grinstein, Left-right SU(4) vector leptoquark model for flavor anomalies, Phys. Rev. D **99**, 055025 (2019).

[47] U. Aydemir, T. Mandal, and S. Mitra, Addressing the $\boldsymbol{R}_{D^{(*)}}$ anomalies with an $\mathbf{S}_1$ leptoquark from $\mathbf{SO(10)}$ grand unification, Phys. Rev. D **101**, 015011 (2020).

[48] C. Cornella, J. Fuentes-Martin, and G. Isidori, Revisiting the vector leptoquark explanation of the B-physics anomalies, J. High Energy Phys. 07 (2019) 168.

[49] O. Popov, M. A. Schmidt, and G. White, R_2 as a single leptoquark solution to $R_{D^{(*)}}$ and $R_{K^{(*)}}$, Phys. Rev. D **100**, 035028 (2019).

[50] I. Bigaran, J. Gargalionis, and R. R. Volkas, A near-minimal leptoquark model for reconciling flavour anomalies and generating radiative neutrino masses, J. High Energy Phys. 10 (2019) 106.

[51] L. Da Rold and F. Lamagna, A vector leptoquark for the B-physics anomalies from a composite GUT, J. High Energy Phys. 12 (2019) 112.

[52] A. Crivellin, D. Müller, and F. Saturnino, Flavor phenomenology of the leptoquark singlet-triplet model, J. High Energy Phys. 06 (2020) 020.

[53] I. Bigaran and R. R. Volkas, Getting chirality right: Single scalar leptoquark solutions to the $(g-2)_{e,\mu}$ puzzle, Phys. Rev. D **102**, 075037 (2020).

[54] W. Altmannshofer, P. S. B. Dev, A. Soni, and Y. Sui, Addressing $\mathrm{R}_{D^{(*)}}$, $\mathrm{R}_{K^{(*)}}$, muon $g-2$ and ANITA anomalies in a minimal R-parity violating supersymmetric framework, Phys. Rev. D **102**, 015031 (2020).

[55] P. S. B. Dev, R. Mohanta, S. Patra, and S. Sahoo, Unified explanation of flavor anomalies, radiative neutrino masses, and ANITA anomalous events in a vector leptoquark model, Phys. Rev. D **102**, 095012 (2020).

[56] A. Crivellin, D. Mueller, and F. Saturnino, Correlating $h \to \mu^+\mu^-$ to the Anomalous Magnetic Moment of the Muon via Leptoquarks, Phys. Rev. Lett. **127**, 021801 (2021).

[57] K. S. Babu, P. S. B. Dev, S. Jana, and A. Thapa, Unified framework for B-anomalies, muon $g-2$ and neutrino masses, J. High Energy Phys. 03 (2021) 179.

[58] A. Angelescu, D. Bečirević, D. A. Faroughy, F. Jaffredo, and O. Sumensari, Single leptoquark solutions to the B-physics anomalies, Phys. Rev. D **104**, 055017 (2021).

[59] T. Nomura and H. Okada, Explanations for anomalies of muon anomalous magnetic dipole moment, $b \to s\mu\mu^-$, and radiative neutrino masses in a leptoquark model, Phys. Rev. D **104**, 035042 (2021).

[60] H. M. Lee, Leptoquark option for B-meson anomalies and leptonic signatures, Phys. Rev. D **104**, 015007 (2021).

[61] M. Du, J. Liang, Z. Liu, and V. Q. Tran, A vector leptoquark interpretation of the muon $g-2$ and B anomalies, arXiv:2104.05685.

[62] K. Ban, Y. Jho, Y. Kwon, S. C. Park, S. Park, and P.-Y. Tseng, A comprehensive study of vector leptoquark on the B-meson and Muon g-2 anomalies, arXiv:2104.06656.

[63] P. S. B. Dev, A. Soni, and F. Xu, Hints of natural supersymmetry in flavor anomalies?, arXiv:2106.15647.

[64] I. Bigaran and R. R. Volkas, Reflecting on chirality: CP-violating extensions of the single scalar-leptoquark solutions for the $(g-2)e,\mu$ puzzles and their implications for lepton EDMs, Phys. Rev. D **105**, 015002 (2022).

[65] G. Bélanger *et al.*, Leptoquark manoeuvres in the dark: A simultaneous solution of the dark matter problem and the R_D anomalies, J. High Energy Phys. 02 (2022) 042.

[66] O. Fischer *et al.*, Unveiling hidden physics at the LHC, arXiv:2109.06065.

[67] W. Buchmüller, R. Ruckl, and D. Wyler, Leptoquarks in lepton—quark collisions, Phys. Lett. B **191**, 442 (1987).

[68] W. Buchmüller and D. Wyler, Effective lagrangian analysis of new interactions and flavor conservation, Nucl. Phys. **B268**, 621 (1986).

[69] B. Grzadkowski, M. Iskrzynski, M. Misiak, and J. Rosiek, Dimension-six terms in the standard model lagrangian, J. High Energy Phys. 10 (2010) 085.
[70] D. Becker *et al.*, The P2 experiment, Eur. Phys. J. A **54**, 208 (2018).
[71] P. S. B. Dev, W. Rodejohann, X.-J. Xu, and Y. Zhang, Searching for Z' bosons at the P2 experiment, J. High Energy Phys. 06 (2021) 039.
[72] B. K. Sahoo, B. P. Das, and H. Spiesberger, New physics constraints from atomic parity violation in cs133, Phys. Rev. D **103**, L111303 (2021).
[73] ATLAS Collaboration, Search for pairs of scalar leptoquarks decaying into quarks and electrons or muons in $\sqrt{s} = 13$ TeV pp collisions with the ATLAS detector, J. High Energy Phys. 10 (2020) 112.
[74] B. Diaz, M. Schmaltz, and Y.-M. Zhong, The leptoquark Hunter's guide: Pair production, J. High Energy Phys. 10 (2017) 097.
[75] ATLAS Collaboration, Search for new non-resonant phenomena in high-mass dilepton final states with the ATLAS detector, J. High Energy Phys. 11 (2020) 005.
[76] A. Crivellin, D. Müller, and L. Schnell, Combined constraints on first generation leptoquarks, Phys. Rev. D **103**, 115023 (2021).
[77] H. Davoudiasl, H.-S. Lee, and W. J. Marciano, 'Dark' Z implications for parity violation, rare meson decays, and Higgs physics, Phys. Rev. D **85**, 115019 (2012).
[78] H. Davoudiasl, H.-S. Lee, and W. J. Marciano, Muon Anomaly and Dark Parity Violation, Phys. Rev. Lett. **109**, 031802 (2012).
[79] J. Erler, C. J. Horowitz, S. Mantry, and P. A. Souder, Weak polarized electron scattering, Annu. Rev. Nucl. Part. Sci. **64**, 269 (2014).
[80] H. Davoudiasl, H.-S. Lee, and W. J. Marciano, Muon $g-2$, rare kaon decays, and parity violation from dark bosons, Phys. Rev. D **89**, 095006 (2014).
[81] V. A. Dzuba, V. V. Flambaum, and Y. V. Stadnik, Probing Low-Mass Vector Bosons with Parity Nonconservation and Nuclear Anapole Moment Measurements in Atoms and Molecules, Phys. Rev. Lett. **119**, 223201 (2017).
[82] M. S. Safronova, D. Budker, D. DeMille, D. F. J. Kimball, A. Derevianko, and C. W. Clark, Search for new physics with atoms and molecules, Rev. Mod. Phys. **90**, 025008 (2018).
[83] Y. Hao, P. Navrátil, E. B. Norrgard, M. Iliaš, E. Eliav, R. G. E. Timmermans *et al.*, Nuclear spin-dependent parity-violating effects in light polyatomic molecules, Phys. Rev. A **102**, 052828 (2020).
[84] B. K. Sahoo and B. P. Das, Constraints on new physics from an improved calculation of parity violation in ^{133}Cs, arXiv:2008.08941.
[85] A. Crivellin, M. Hoferichter, M. Kirk, C. A. Manzari, and L. Schnell, First-generation new physics in simplified models: From low-energy parity violation to the LHC, J. High Energy Phys. 10 (2021) 221.
[86] I. Brivio and M. Trott, The standard model as an effective field theory, Phys. Rep. **793**, 1 (2019).
[87] A. Falkowski, M. González-Alonso, and K. Mimouni, Compilation of low-energy constraints on 4-fermion operators in the SMEFT, J. High Energy Phys. 08 (2017) 123.
[88] R. Boughezal, F. Petriello, and D. Wiegand, Disentangling SMEFT operators with future low-energy PVES experiments, Phys. Rev. D **104**, 016005 (2021).
[89] E. Del Nobile, Appendiciario—A hands-on manual on the theory of direct dark matter detection, arXiv:2104.12785.
[90] M. Hoferichter, J. Menéndez, and A. Schwenk, Coherent elastic neutrino-nucleus scattering: EFT analysis and nuclear responses, Phys. Rev. D **102**, 074018 (2020).
[91] C. J. Horowitz, Weak radius of the proton, Phys. Lett. B **789**, 675 (2019).
[92] R. H. Helm, Inelastic and elastic scattering of 187-Mev electrons from selected even-even nuclei, Phys. Rev. **104**, 1466 (1956).
[93] D. K. Papoulias, COHERENT constraints after the COHERENT-2020 quenching factor measurement, Phys. Rev. D **102**, 113004 (2020).
[94] CONUS Collaboration, Novel constraints on neutrino physics beyond the standard model from the CONUS experiment, arXiv:2110.02174.
[95] I. Bischer and W. Rodejohann, General neutrino interactions from an effective field theory perspective, Nucl. Phys. **B947**, 114746 (2019).
[96] K. S. Kumar, S. Mantry, W. J. Marciano, and P. A. Souder, Low energy measurements of the weak mixing angle, Annu. Rev. Nucl. Part. Sci. **63**, 237 (2013).
[97] A. I. Milstein and O. P. Sushkov, Parity nonconservation in heavy atoms: The radiative correction enhanced by the strong electric field of the nucleus, Phys. Rev. A **66**, 022108 (2002).
[98] A. I. Milstein, O. P. Sushkov, and I. S. Terekhov, Radiative Corrections and Parity Nonconservation in Heavy Atoms, Phys. Rev. Lett. **89**, 283003 (2002).
[99] CMS Collaboration, Search for contact interactions and large extra dimensions in the dilepton mass spectra from proton-proton collisions at $\sqrt{s} = 13$ TeV, J. High Energy Phys. 04 (2019) 114.
[100] J. Alwall, R. Frederix, S. Frixione, V. Hirschi, F. Maltoni, O. Mattelaer *et al.*, The automated computation of tree-level and next-to-leading order differential cross sections, and their matching to parton shower simulations, J. High Energy Phys. 07 (2014) 079.
[101] N. D. Christensen and C. Duhr, FeynRules—Feynman rules made easy, Comput. Phys. Commun. **180**, 1614 (2009).
[102] A. Alloul, N. D. Christensen, C. Degrande, C. Duhr, and B. Fuks, FeynRules 2.0—A complete toolbox for tree-level phenomenology, Comput. Phys. Commun. **185**, 2250 (2014).